Published in final edited form as:
Am J Surg Pathol. 2012 June ; 36(6): 818–830. doi:10.1097/PAS.0b013e3182498be5.

A distinct subset of Atypical Spitz Tumors is characterized by *BRAF* mutation and loss of BAP1 expression

Thomas Wiesner[1,3,*], **Rajmohan Murali**[1,2,*], **Isabella Fried**[3], **Lorenzo Cerroni**[3], **Klaus Busam**[2], **Heinz Kutzner**[4], and **Boris C. Bastian**[1,2,5]

[1]Human Oncology and Pathogenesis Program, Memorial Sloan-Kettering Cancer Center, New York, USA

[2]Department of Pathology, Memorial Sloan-Kettering Cancer Center, New York, USA

[3]Department of Dermatology, Medical University of Graz, Graz, Austria

[4]Dermatopathologie Friedrichshafen, Friedrichshafen, Germany

[5]Departments of Dermatology and Pathology and Helen Diller Family Comprehensive Cancer Center, University of California San Francisco, San Francisco, USA

Abstract

We recently reported that germline mutations in *BAP1* cause a familial tumor syndrome characterized by high penetrance for melanocytic tumors with distinct clinical and histologic features. Melanocytic neoplasms in affected individuals harbored *BRAF* mutations, showed loss of BAP1 expression, and histologically resembled so-called “atypical Spitz tumors” (ASTs). ASTs are an ill-defined and probably heterogenous group of melanocytic tumors that display histologic features seen in both Spitz nevi and melanomas. Their biological behavior cannot be reliably predicted. In view of the histologic similarities of the familial tumors and ASTs, we hypothesized that a subset of ASTs might harbor genetic alterations seen in the familial tumors. To address this hypothesis, we analyzed 32 sporadic ASTs for *BRAF* mutations and for BAP1 expression. Nine (28%) sporadic ASTs showed loss of BAP1 expression, of which 8 (89%) had concomitant *BRAF* mutations. Only 1 of the BAP1-positive ASTs (4%) had a *BRAF* mutation (P<0.0001). *BRAF*-mutated, BAP1-negative tumors were primarily located in the dermis and were composed entirely or predominantly of epithelioid melanocytes with abundant amphophilic cytoplasm and well-defined cytoplasmic borders. Nuclei were commonly vesicular and exhibited substantial pleomorphism and conspicuous nucleoli. The combination of *BRAF* mutation and loss of nuclear BAP1 expression thus characterizes a subset of ASTs with distinct histologic features. The typical morphology of these tumors and BAP1 immunohistochemistry provide pathologic clues that will enable accurate identification of this subset. Future studies are necessary to determine whether this subset has a predictable clinical behavior.

Since the recognition of Spitz nevi, pathologists have increasingly identified a group of melanocytic tumors that exhibit histologic features overlapping those of Spitz nevi and melanomas. These tumors are often referred to as ‘atypical Spitz tumors’ (ASTs) and are likely to represent a heterogenous group of tumors that share some morphologic similarities. ASTs may cause diagnostic problems because their unequivocal histologic separation into

Address for correspondence, **Thomas Wiesner, MD**, Human Oncology and Pathogenesis Program, Memorial Sloan-Kettering Cancer Center, 1275 York Avenue, Box 20, New York, NY 10065, USA, wiesnert@mskcc.org, **Boris Bastian, MD**, Dermatopathology Section, Departments of Dermatology and Pathology, San Francisco, CA 94143, USA, Phone: 415-353-7550 Boris.Bastian@ucsf.edu.
*contributed equally

Spitz nevi and spitzoid melanoma is not always possible, as demonstrated by a significant lack of interobserver agreement, even among experts.[1,2,5] Recently, we described an autosomal dominant tumor syndrome caused by inactivating germline mutations of the *BAP1* gene.[16] Affected individuals had multiple cutaneous spitzoid melanocytic neoplasms and were predisposed to increased risk of developing cutaneous and uveal melanoma.[16] The characteristic cutaneous melanocytic tumors were skin-colored papules or nodules. Histologically, they were composed of dermal aggregates of epithelioid melanocytes with abundant amphophilic cytoplasm, pleomorphic vesicular nuclei, and conspicuous nucleoli. The majority of tumors lost the remaining wild-type *BAP1* allele by various somatic alterations and lacked immunohistochemical expression of BAP1 (Fig. 1).[16]

Although many of the cytologic features of the tumor cells were reminiscent of epithelioid cells of Spitz nevi, other features characteristically present in Spitz nevi (eg, clefting around junctional melanocytic nests, spindle-shaped melanocytes, epidermal hyperplasia, hypergranulosis, and Kamino bodies)[6] were consistently absent. Furthermore, the vast majority of familial BAP1-negative neoplasms showed $BRAF^{V600E}$ mutations,[16] which are typically absent in Spitz nevi.[9] The characteristic morphology and distinct genetic aberrations in the familial melanocytic tumors suggested that these neoplasms constitute a distinct category of melanocytic tumors. In this study, we analyzed a series of ASTs with no known family history to determine whether histologic features, BAP1 expression, and mutation status of *BRAF* or *HRAS* are helpful in subclassifying this challenging category of melanocytic neoplasms.

METHODS

Specimens

The study was approved by the Ethics Committees of the Medical University of Graz (Graz, Austria), and by the Memorial Sloan-Kettering Cancer Center (New York) and was conducted according to the Declaration of Helsinki. Specimens were fixed in 4% buffered formalin, routinely processed, and embedded in paraffin. Sections of 4 mm thickness were stained routinely with hematoxylin and eosin for histologic evaluation.

Two sets of cases were collected. The evaluation set for BAP1 immunohistochemistry (IHC) consisted of 46 positive controls (29 common acquired nevi and 17 classical Spitz nevi showing no *BAP1* mutations) and 42 negative controls (epithelioid melanocytic tumors from 2 families with *BAP1* germline mutations; 29 tumors from family 1 and 13 tumors from family 2, as described in Wiesner et al[16]). The independent test set of 32 sporadic ASTs with epithelioid cytomorphology was collected from the diagnostic files and consultation cases of the authors. The sequencing and clinical data of the evaluation set and of 2 of the ASTs (cases 6 and 7 in Table 1) have been published previously.[16] Available clinical and pathologic characteristics of the tumors are summarized in Table 1.

BAP1 immunohistochemistry

In the evaluation set, we assessed expression of BAP1 by immunohistochemistry (IHC) to determine its specificity and sensitivity. IHC was performed with an automated IHC system (Ventana BenchMark XT, Ventana Medical Systems, Inc., Tucson, AZ) using an alkaline phosphatase method and a red chromogen, according to the manufacturer's instructions. Briefly, following deparaffinization of paraffin tissue sections and heat-induced antigen retrieval, the sections were incubated with BAP1 antibody (clone C-4, 1:50 dilution, Santa Cruz Biotechnology, Inc., Santa Cruz, CA) for 1 hour. A subsequent amplification step was followed by incubation with Hematoxylin II counterstain for 4 minutes and then with blueing reagent for 4 minutes. Nuclei of keratinocytes of the epidermis and appendages,

fibroblasts and lymphocytes served as internal controls for BAP1 expression. Tumors were scored as positive or negative depending on whether or not their nuclei stained with BAP1.

DNA extraction and Sanger sequencing

Tumor and non-tumor areas were separately microdissected from sections of archival paraffin-embedded tissue using a dissection microscope. DNA was extracted and purified with a QIAamp DNA FFPE Tissue Kit (Qiagen, Hilden, Germany) according to the manufacturer's instructions.

Mutations in *BAP1* (all exons), *BRAF* (exon 15), and *HRAS* (exons 1 and 2) were determined by direct sequencing using previously described primers.[3,16] The PCR reaction conditions were 0.25 mM dNTPs, 0.4. BSA (New England Biolabs), 1 U Hotstar Taq (Qiagen), 1× Hotstar Taq buffer (Qiagen) and 0.4 μM primer. PCR consisted of 35 cycles of 95 °C (45 s), 57 °C (45 s) and 72 °C (45 s) after initial denaturation at 95 °C for 5 min. PCR reaction products were purified with the QIAquick PCR Purification kit (Qiagen) and then used as templates for sequencing in both directions using Big Dye v3.1 (Applied Biosystems). Dye terminators were removed using the CleanSEQ kit (Agencourt Biosciences), and subsequent products were run on the ABI PRISM 3730×l (Applied Biosystems). Mutations were identified by using Sequencher 5.0 software (Gene Codes Corporation, Ann Arbor, MI) and only considered when variants were called in reads in both directions. Normal DNA was sequenced from the adjacent non-tumor tissue to determine whether the mutations were somatically acquired or germline.

Array-based Comparative Genomic Hybridization

BAP1-negative cases in which sufficient DNA was available, were analyzed using array-based comparative genomic hybridization (CGH). DNA was labeled using the Bioprime Array CGH Genomic Labeling Kit according to the manufacturer's instructions (Invitrogen, Carlsberg, CA) as described previously.[15] Briefly, 500ng test and reference DNA (Promega, Madison, WI) were differentially labeled with dCTP-Cy5 and dCTP-Cy3, respectively (GE Healthcare, Piscataway, NJ). Genome-wide analysis of DNA copy number changes was conducted using an oligonucleotide array containing 60,000 probes according to the manufacturer's protocol version 6.0 (Agilent, Santa Clara, CA). Slides were scanned using Agilent's microarray scanner G2505B and analyzed using Agilent Feature Extraction and DNA Workbench software 6.5.018.

RESULTS

Accuracy of IHC to Determine BAP1 Status

As negative controls (cases with functional loss of BAP1) we used the 42 epithelioid melanocytic tumors from *BAP1* germline mutation carriers. Of these, 33 (79%) tumors showed bi-allelic loss of *BAP1* (inactivating germline mutation combined with either somatic deletion, loss of heterozygosity, or mutation of the remaining wild-type allele).[16] All 33 cases (100%) with bi-allelic loss of *BAP1* were IHC negative. The remaining 9 (21%) of these 42 cases had a very similar histologic appearance, but no detectable somatically acquired alteration of *BAP1* (no somatic deletion, loss of heterozygosity, or mutation). All of these 9 cases also showed loss of BAP1 IHC expression, indicating that the wild-type *BAP1* allele had been silenced in a way not detected by our analysis. Internal controls consisting of the nuclei of non-tumor cells (keratinocytes and lymphocytes) confirmed that the IHC procedure was working (Fig. 1E).

Our positive control set consisted of 29 commonly acquired melanocytic nevi and 17 conventional Spitz nevi, in which we did not find any *BAP1* mutations in our previous

study.[16] All of these cases showed strong nuclear BAP1 staining. These results indicate that BAP1 IHC may be a convenient method for assessing the functional status of BAP1.

Loss of BAP1 Expression by IHC Identifies a Morphologically Distinct Subset of Tumors

The 32 ASTs selected for this study showed histologic features overlapping those of Spitz nevus and melanoma. Concern for malignancy was raised by the presence of varying combinations of atypical features such as architectural asymmetry, increased cellularity, nuclear pleomorphism, nucleolar prominence, and detectable mitotic figures (Table 1).

BAP1 IHC was negative in 9 (28%) cases. The BAP1-negative tumors were predominantly or exclusively intradermal (Figs. 2A, 3A, 4A, 5A, 6A), whereas 11 of 23 (48%) BAP1-positive tumors had a significant junctional component. Additional features shared by BAP1-negative tumors were the predominance of plump epithelioid cells with moderate to large amounts of amphophilic cytoplasm and very well-demarcated cytoplasmic borders (Figs. 2B, 3B, 4B, 5C, 6B). Their nuclei were round or oval in shape and exhibited moderate pleomorphism with vesicular chromatin and often conspicuous nucleoli. There were also scattered giant cells, some of which were multinucleated (Figs. 2C, 3C, 5C). In 3 of the 9 BAP1-negative cases (33%), significant numbers of tumor-infiltrating lymphocytes (TILs) were identified, resulting in a histologic appearance resembling that seen in so-called “halo Spitz nevus” (Figs. 2, 3). Occasionally, aggregates of tumor cells were separated by delicate bands of collagen, but prominent fibrosis or sclerosis was not a feature.

Several statistically significant differences between BAP1-negative and BAP1-positive tumors were observed. BAP1-negative neoplasms were located more frequently on the trunk and less often on the limbs, and were less mitotically active. They more often demonstrated sheet-like growth, contained amphophilic cytoplasm with well-defined cytoplasmic borders and marked TILs, and were less often composed of spindle-shaped or oval cells. Nuclear chromatin was more commonly vesicular, and binucleation and multinucleation were more frequently seen. Although these differences were statistically significant, many of the cytologic features seen in the BAP1-negative tumors were also identified to varying degrees in some BAP1-positive tumors (Table 2).

Mutations and Deletions of BAP1

BAP1 was sequenced in all 9 BAP1-negative cases, and somatically acquired mutations were found in 5 cases (56%, Table 3); 2 were frameshift mutations (Figs. 2F, 4E), 2 were nonsense mutations (Fig. 6C), and 1 was a missense mutation (Fig. 5F). The 2 frameshift mutations and 2 nonsense mutations resulted in premature termination of the protein. No mutations were found in the remaining 4 BAP1-negative cases and in 20 of 23 BAP1-positive cases. In the remaining 3 BAP1-positive cases (case # 12, 14, and 15 in Table 1), *BAP1* could not be fully sequenced. Array CGH was performed in 4 of the cases with negative BAP1 IHC. In 1 case that had a *BAP1* frameshift mutation there was focal loss of the *BAP1* locus at 3p21 (Fig. 4C). Another case that bore a *BAP1* missense mutation (Fig. 5F) was characterized by loss of the entire chromosome 3 (Fig. 5D). The remaining 2 cases showed no copy number changes of *BAP1* or elsewhere in the genome (Fig. 6D).

Mutations of BRAF and HRAS

BRAF and *HRAS* were sequenced in 31 ASTs. Nine (29%) tumors carried a $BRAF^{V600E}$ mutation whereas no *HRAS* mutations were found (Figs. 2E, 4D, 6C, Table 1). There was a significant association between *BRAF* mutation status and loss of BAP1 by IHC. Eight of the 9 (89%) $BRAF^{V600E}$-mutant tumors showed loss of BAP1 expression by IHC (Table 1, Fisher exact test: $P<0.0001$), suggesting that *BRAF* mutation and *BAP1* loss characterizes a distinct subset of ASTs. Only 1 of the 9 *BRAF*-mutated cases showed strong expression of

BAP1. In this case, the tumor was cellular and was composed of sheets of spindle-shaped, oval, and epithelioid melanocytes with vesicular nuclei and amphophilic cytoplasm but lacking well-defined cytoplasmic borders (Fig. 7).

DISCUSSION

Traditional classification systems for melanocytic neoplasms rely on clinical and histologic characteristics to describe subtypes of nevi (eg, acquired nevi, congenital nevi, Spitz nevi, blue nevi) and melanomas (eg, superficial spreading melanomas, nodular melanomas, acral lentiginous melanomas, lentigo maligna melanomas). More recently, acquired mutations in oncogenes that lead to constitutive activation of critical signaling pathways have provided additional information useful for classification. These include *BRAF* mutations that are frequent in common acquired nevi[10] and in melanomas from skin without chronic sun-induced damage[8]; KIT mutations in acral and mucosal melanoma and melanomas on skin with chronic sun-induced damage[7]; *HRAS* mutations in a subset of Spitz nevi[3]; and *GNAQ* and *GNA11* mutations in blue nevi and uveal melanoma.[12,13] Integration of underlying genetic aberrations and clinicopathologic features can lead to refined ways to classify melanocytic neoplasms and improve clinical relevance by incorporating information that can guide selection of targeted therapeutic agents.[14]

Here, we shed further light on the heterogenous group of ASTs by demonstrating that they appear to be composed of biologically distinct entities. In the present study, we have identified a histologically distinct subset of ASTs characterized by $BRAF^{V600E}$ mutations and loss of BAP1 expression. In all cases, *BAP1* loss was somatically acquired without evidence of a preexisting germline mutation. These results demonstrate that melanocytic neoplasms with *BAP1* alterations can occur outside of the previously described tumor predisposition syndrome caused by germline *BAP1* mutations. We have also shown that *BAP1* status can be reliably identified by IHC, which will make BAP1 IHC a useful tool for subtyping melanocytic neoplasms. Our observation that a greater number of tumors exhibited loss of BAP1 protein expression by IHC compared with *BAP1* deletions or mutations indicates that BAP1 may become functionally inactivated by mechanisms other than deletions or mutations in the coding region; for example, epigenetic changes leading to silencing of the *BAP1* gene or other, yet to be identified, alterations that prevent BAP1 expression. Detailed in vitro and in vivo studies are needed to investigate the correlation between nuclear BAP1 protein expression (assessed by IHC) and BAP1 functional activity.

The sporadic $BRAF^{V600E}$/$BAP1^{neg}$ tumors exhibited a typical epithelioid histomorphology that was previously seen in the BAP1-negative melanocytic skin tumors in patients with *BAP1* germline mutations.[16] The cytologic appearances of $BRAF^{V600E}$/$BAP1^{neg}$ tumors (plump epithelioid cells with amphophilic cytoplasm and very well-demarcated cytoplasmic borders, moderately pleomorphic round/oval nuclei with vesicular chromatin and variably conspicuous nucleoli, and multinucleate/giant cells) were distinctive but were not absolutely specific, as some features were also identified to varying degrees in some BAP1-positive tumors. Similarly, architectural features and stromal alterations absolutely specific to BAP1-negative tumors were not identified. TILs were prominent in many BAP1-negative tumors, but this was also not a specific diagnostic feature.

We previously reported that another subset of ASTs is characterized by *HRAS* mutations, copy number increases of chromosome 11p, and distinct microscopic features.[3,11] These tumors had similar cytologic features to those described here and were also predominantly intradermal. In contrast to the $BRAF^{V600E}$/$BAP1^{neg}$ tumors, the *HRAS* mutant neoplasms were associated with marked desmoplasia and did not show densely cellular aggregates. These results indicate that $BRAF^{V600E}$ mutations and loss of BAP1 defines an additional

genetic/morphologic subset of epithelioid ASTs (8/32, 25%). Thus, to date, spitzoid tumors are composed of 3 distinguishable categories, *HRAS* mutant, $BRAF^{V600E}$/$BAP1^{neg}$ tumors, and a (probably still heterogeneous) category of tumors with as yet unknown genetic characteristics.

Unfortunately, we did not have follow-up information on the tumors analyzed in our study; hence, we cannot address the important question of whether *BAP1* or *BRAF* status provides any prognostic information about the tumors. In our experience, patients with ASTs almost invariably have an uneventful follow-up.[4] Only a small minority develop widespread metastasis, raising the possibility that they were melanoma from the outset. Future studies are necessary to determine which, if any, genetic or morphologic criteria identified in this study can help in the risk assessment of these tumors.

In conclusion, we have described a distinct subset of ASTs characterized by loss of BAP1 expression, $BRAF^{V600E}$ mutations, and some distinct histologic features. Our findings establish a platform for future studies to investigate the prognostic significance of genetically defined subsets of ASTs.

REFERENCES

1. Barnhill RL. The Spitzoid lesion: rethinking Spitz tumors, atypical variants, 'Spitzoid melanoma' and risk assessment. Mod Pathol. 2006; 19(Suppl 2):S21–S33. [PubMed: 16446713]
2. Barnhill RL, Argenyi ZB, From L, et al. Atypical Spitz nevi/tumors: lack of consensus for diagnosis, discrimination from melanoma, and prediction of outcome. Hum Pathol. 1999; 30:513–520. [PubMed: 10333219]
3. Bastian BC, LeBoit PE, Pinkel D. Mutations and copy number increase of *HRAS* in Spitz nevi with distinctive histopathological features. Am J Pathol. 2000; 157:967–972. [PubMed: 10980135]
4. Busam KJ, Murali R, Pulitzer M, et al. Atypical spitzoid melanocytic tumors with positive sentinel lymph nodes in children and teenagers, and comparison with histologically unambiguous and lethal melanomas. Am J Surg Pathol. 2009; 33:1386–1395. [PubMed: 19609204]
5. Cerroni L, Barnhill R, Elder D, et al. Melanocytic tumors of uncertain malignant potential: results of a tutorial held at the XXIX Symposium of the International Society of Dermatopathology in Graz, October 2008. Am J Surg Pathol. 2010; 34:314–326. [PubMed: 20118771]
6. Crotty KA. Spitz naevus: histological features and distinction from malignant melanoma. Australasian Journal of Dermatology. 1997; 38(Suppl 1):S49–S53. [PubMed: 10994473]
7. Curtin JA, Busam K, Pinkel D, et al. Somatic activation of KIT in distinct subtypes of melanoma. J Clin Oncol. 2006; 24:4340–4346. [PubMed: 16908931]
8. Curtin JA, Fridlyand J, Kageshita T, et al. Distinct sets of genetic alterations in melanoma. N Engl J Med. 2005; 353:2135–2147. [PubMed: 16291983]
9. Palmedo G, Hantschke M, Rutten A, et al. The T1796A mutation of the *BRAF* gene is absent in Spitz nevi. J Cutan Pathol. 2004; 31:266–270. [PubMed: 14984580]
10. Pollock PM, Harper UL, Hansen KS, et al. High frequency of *BRAF* mutations in nevi. Nat Genet. 2003; 33:19–20. [PubMed: 12447372]
11. van Engen-van Grunsven AC, van Dijk MC, Ruiter DJ, et al. *HRAS*-mutated Spitz tumors: A subtype of Spitz tumors with distinct features. Am J Surg Pathol. 2010; 34:1436–1441. [PubMed: 20871217]
12. Van Raamsdonk CD, Bezrookove V, Green G, et al. Frequent somatic mutations of *GNAQ* in uveal melanoma and blue naevi. Nature. 2009; 457:599–602. [PubMed: 19078957]
13. Van Raamsdonk CD, Griewank KG, Crosby MB, et al. Mutations in *GNA11* in uveal melanoma. N Engl J Med. 2010; 363:2191–2199. [PubMed: 21083380]
14. Whiteman DC, Pavan WJ, Bastian BC. The melanomas: a synthesis of epidemiological, clinical, histopathological, genetic, and biological aspects, supporting distinct subtypes, causal pathways, and cells of origin. Pigment Cell Melanoma Res. 2011; 24:879–897. [PubMed: 21707960]

15. Wiesner T, Obenauf AC, Cota C, et al. Alterations of the cell-cycle inhibitors p27(KIP1) and p16(INK4a) are frequent in blastic plasmacytoid dendritic cell neoplasms. J Invest Dermatol. 2010; 130:1152–1157. [PubMed: 19924135]

16. Wiesner T, Obenauf AC, Murali R, et al. Germline mutations in BAP1 predispose to melanocytic tumors. Nat Genet. 2011; 43:1018–1021. [PubMed: 21874003]

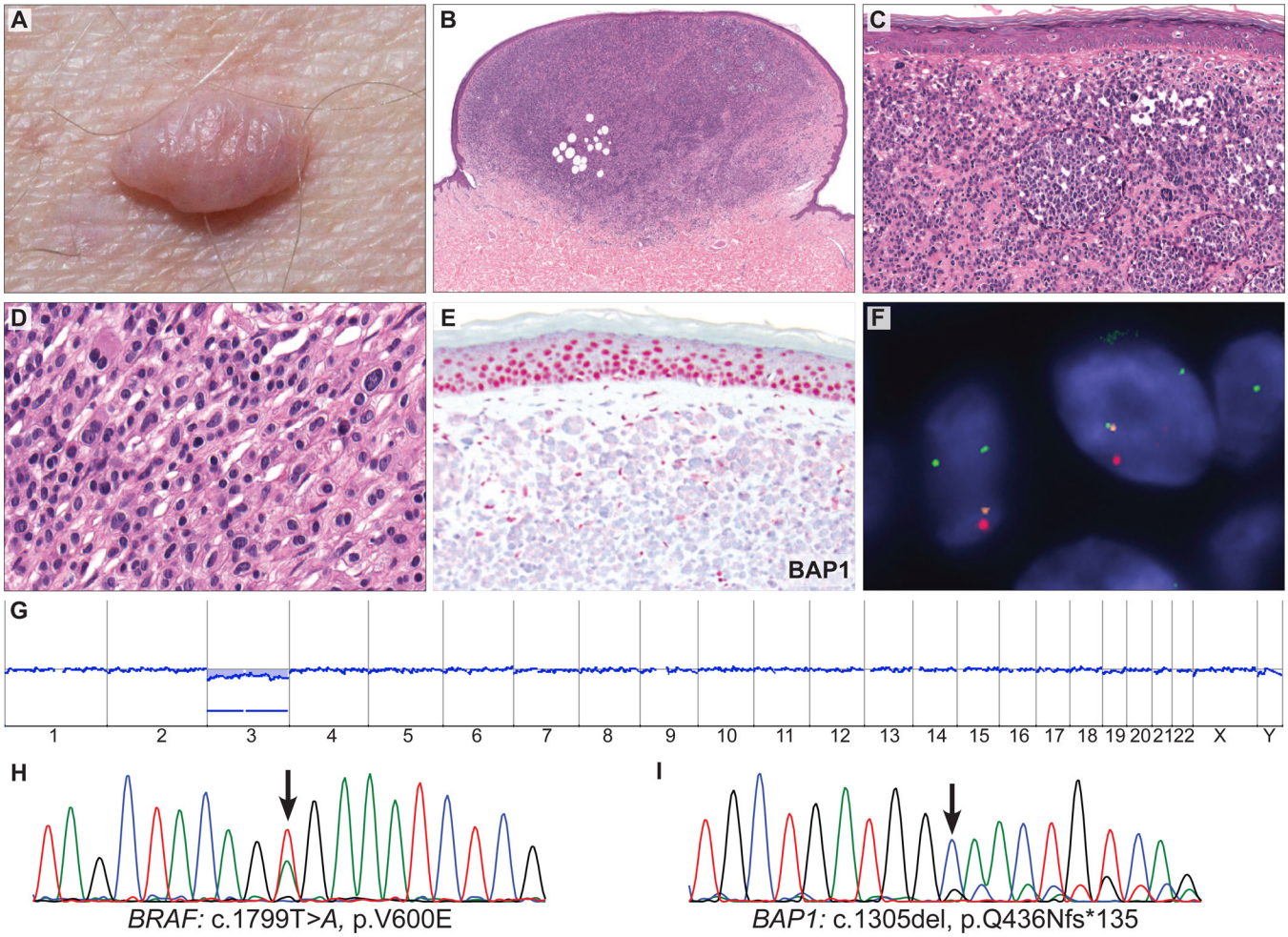

FIGURE 1.

Skin tumor from a 49-year-old man harboring a germline mutation in *BAP1*. **A**, Dome-shaped to pedunculated, skin-colored tumor. **B**, Polypoid, relatively symmetrical, dermal tumor consisting of (**C**) melanocytes arranged in nests and sheets. **D**, The neoplastic cells are characterized by moderate amounts of amphophilic cytoplasm, well-defined cytoplasmic borders, and pleomorphic oval nucleoli. **E**, BAP1 IHC is negative in tumor cells but positive in epidermal keratinocyte nuclei and in scattered lymphocytes within the tumor. **F**, Fluorescence in situ hybridization shows loss of the second *BAP1* allele in tumor cell nuclei: 1 red signal (chr. 3p21, *BAP1* locus), 1 orange signal (chr. 3p25), and 2 green control signals per nucleus. **G**, Array CGH shows a loss of the whole chromosome 3 with no other chromosomal aberrations. **H**, The sequencing electropherograms show a $BRAF^{V600E}$ mutation and (**I**) the germline *BAP1* mutation. The wild-type *BAP1* sequence is markedly reduced indicating a loss of the wild-type allele in the tumor.

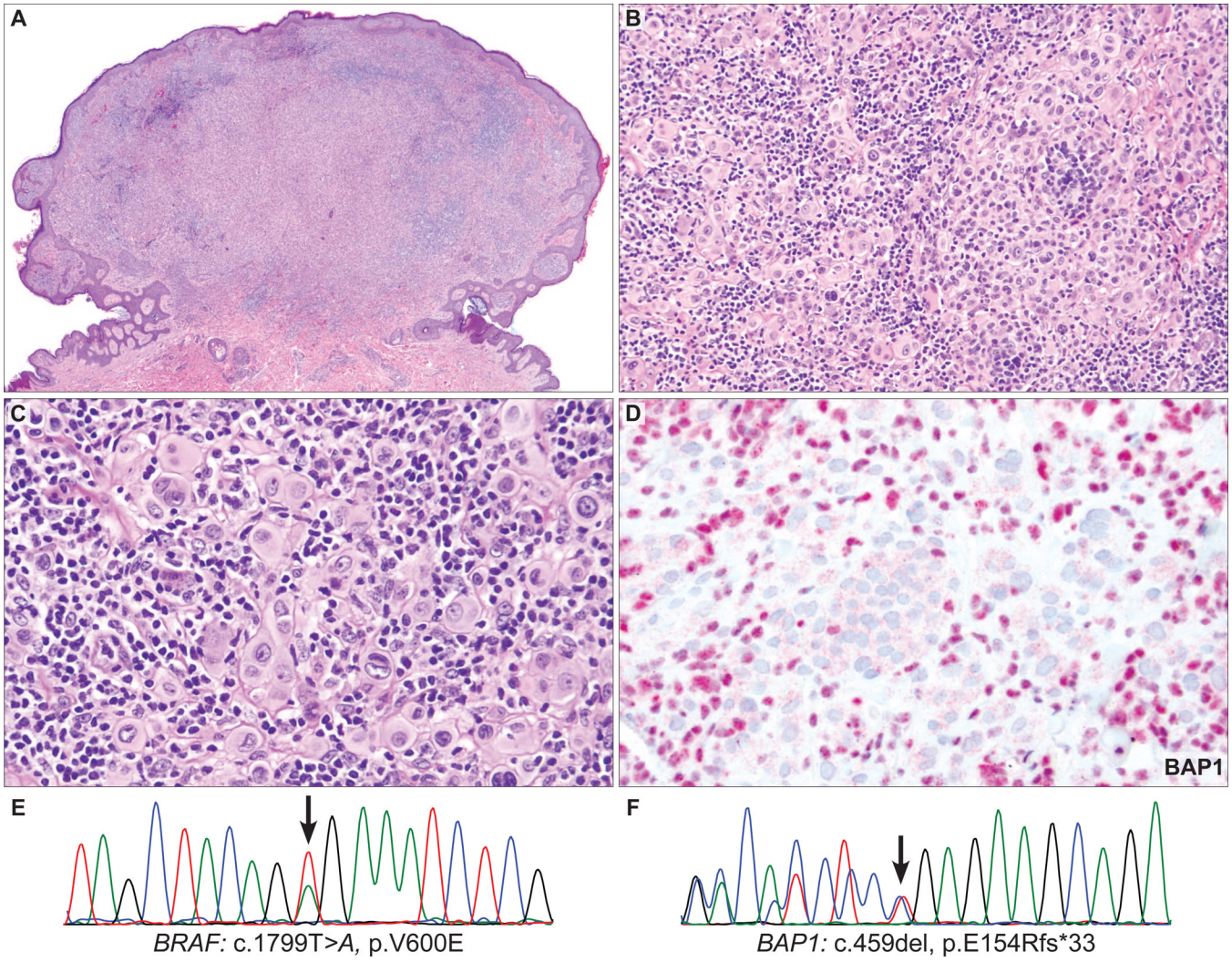

FIGURE 2.

AST from the shoulder of a 23-year-old man (case 1). **A**, Polypoid, predominantly dermal melanocytic tumor composed of (**B**) large epithelioid cells with numerous admixed lymphocytes. **C**, The tumor cells contain abundant amphophilic cytoplasm with well-defined cytoplasmic borders and pleomorphic, round-to-oval, vesicular nuclei with conspicuous nucleoli. TILs are prominent. **D**, The epithelioid cells do not express BAP1, whereas the admixed lymphocytes are strongly positive for BAP1. **E**, Sequencing electropherograms show a $BRAF^{V600E}$ mutation and (**F**) an inactivating, frameshift *BAP1* mutation (c.459del, p.E154Rfs*33) in the tumor.

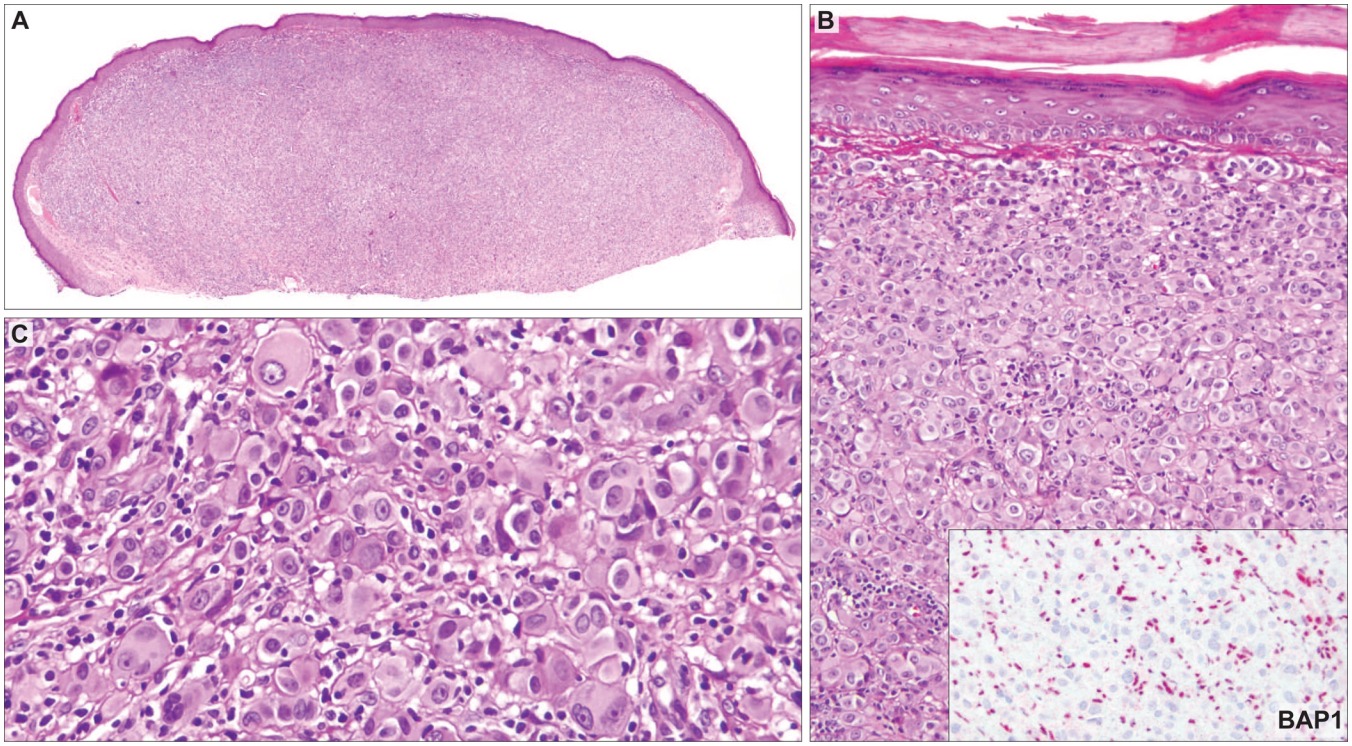

FIGURE 3.

AST from the back of 19-year-old patient (case 2). **A**, Shave biopsy of a relatively symmetric dermal tumor composed of (**B**) sheets and nests of large epithelioid cells. Inset: No BAP1 staining in the nuclei of epithelioid cells, whereas the admixed lymphocytes are strikingly positive. **C**, The tumor cells contain abundant amphophilic cytoplasm with well-defined cytoplasmic borders and very pleomorphic round/oval vesicular nuclei with conspicuous nucleoli. Occasional multinucleate tumor cells are present. Note the prominent TILs.

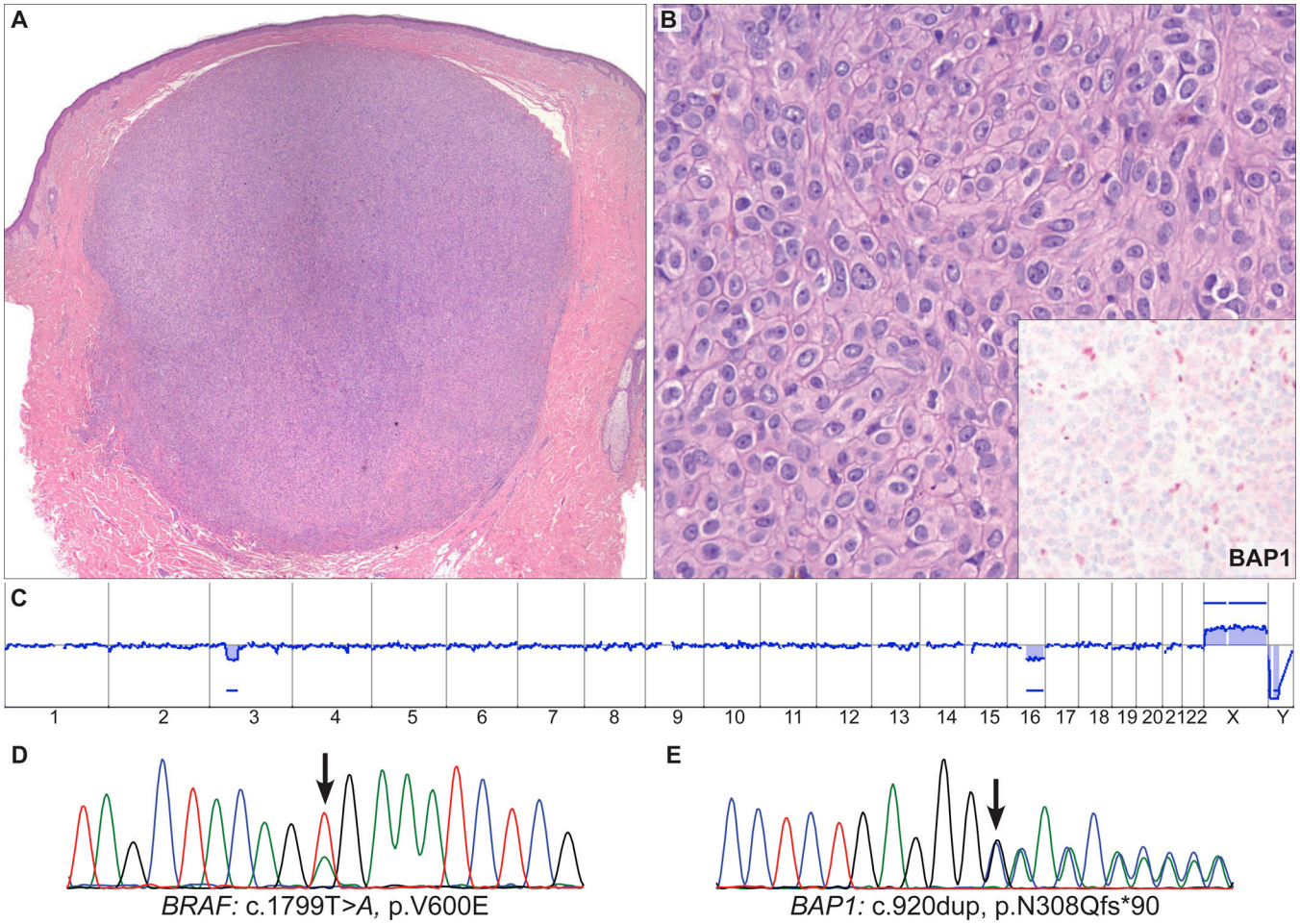

FIGURE 4.

AST from the upper back of 51-year-old woman (case 8). **A**, Symmetrical dermal tumor composed of (**B**) sheets of large epithelioid cells. The tumor cells contain abundant amphophilic cytoplasm with well-defined cytoplasmic borders and pleomorphic vesicular nuclei with conspicuous nucleoli. Occasional multinucleate tumor cells are present. Only few TILs are present. Inset: Absent nuclear staining for BAP1 in the epithelioid cells, with some positive admixed lymphocytes. **C**, Array CGH of the tumor shows a focal loss of the *BAP1* region on chr. 3 and a loss of the long arm of chr. 16. **D**, The sequencing electropherograms show a $BRAF^{V600E}$ mutation and (**E**) an inactivating frameshift mutation of *BAP1* (c.920dup, p.N308Qfs*90).

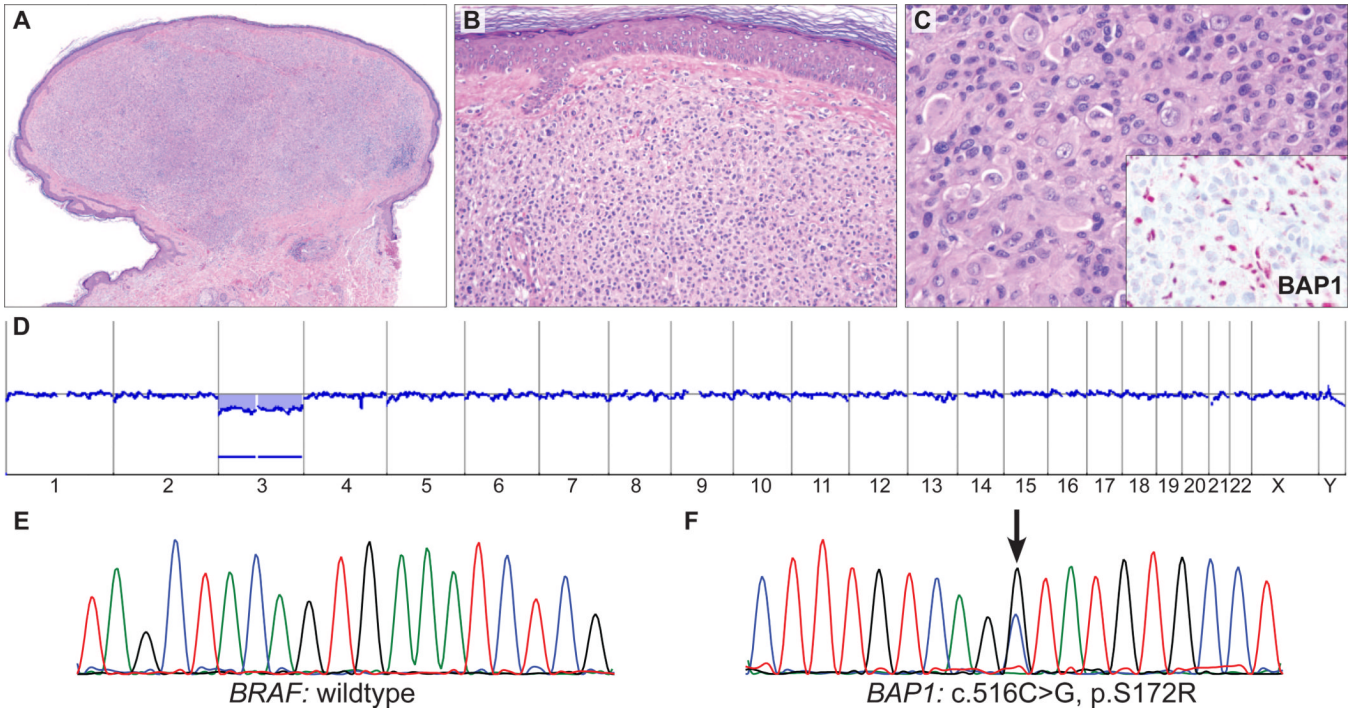

FIGURE 5.

AST from a 59-year-old man (case 9). **A**, Symmetrical, melanocytic tumor (**B**) with no epidermal involvement. **C**, Medium-to-large epithelioid cells with abundant amphophilic cytoplasm and pleomorphic, vesicular nuclei with conspicuous nucleoli. Inset: Absent nuclear BAP1 staining in large epithelioid melanocytes with strong nuclear staining in admixed lymphocytes. **D**, Array CGH shows a loss of the whole chromosome 3 with no other chromosomal aberrations. **E**, Sequencing revealed no *BRAF*^{V600E} mutation (wild type) but (**F**) a missense *BAP1* mutation (c.516C > G, p.S172R) in the tumor.

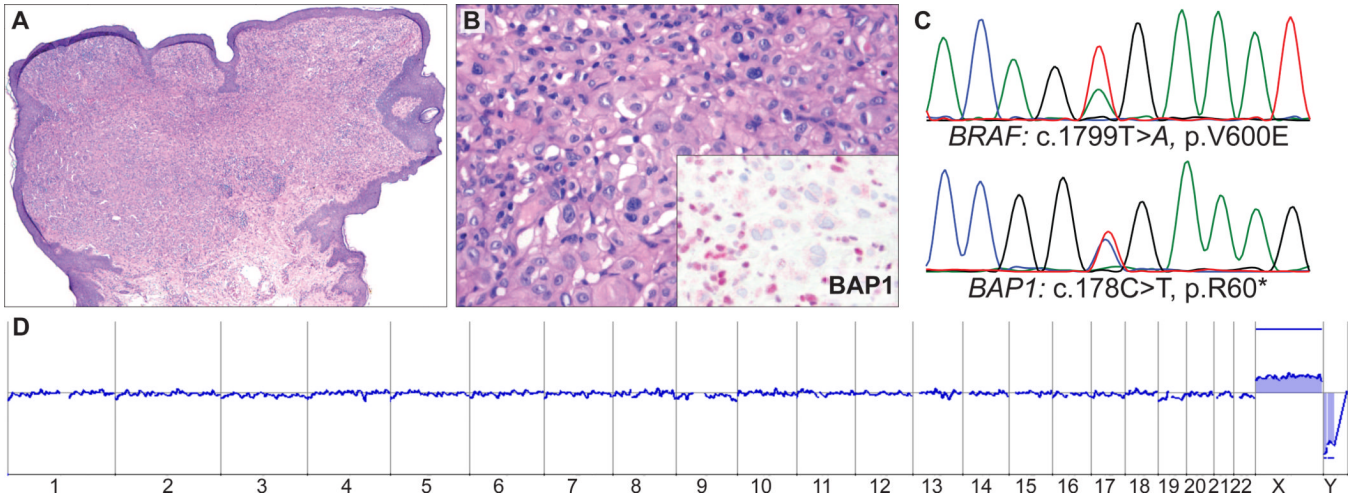

FIGURE 6.

AST from the upper back of a 44-year-old woman (case 6). **A**, Small polypoid melanocytic tumor (**B**) with medium-to-large epithelioid cells and admixed lymphocytes. Inset: Absent BAP1 staining in melanocytes but strong nuclear staining in admixed lymphocytes. **C**, Sequencing electropherograms show a $BRAF^{V600E}$ mutation and an inactivating, nonsense mutation of *BAP1* (c.178C > T, p.R60*). **D**, Array CGH shows a balanced profile with no gains and losses.

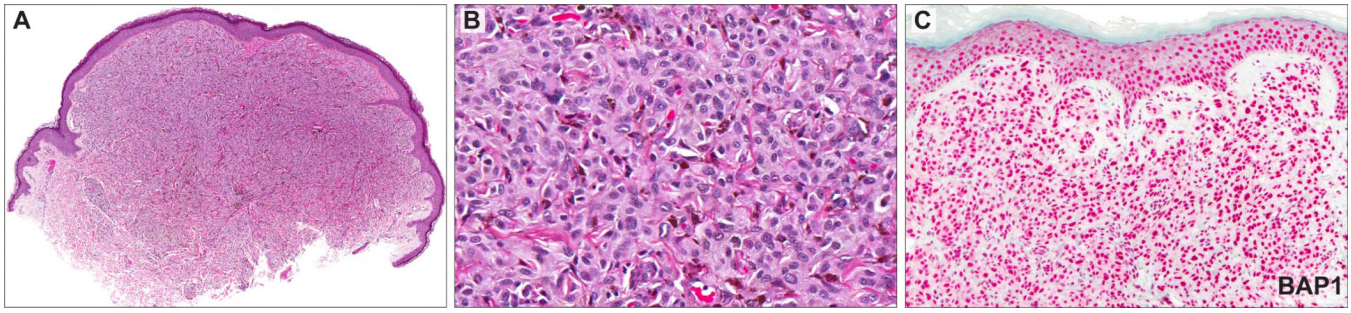

FIGURE 7.

AST from the arm of a 37-year-old patient (case 10). **A**, Dome-shaped melanocytic tumor (**B**) composed of sheets of medium-sized, spindle-shaped, oval, and epithelioid melanocytes with amphophilic cytoplasm but lacking distinct cytoplasmic borders. **C**, Strong expression of BAP1 in keratinocytes and melanocytes. This tumor showed a $BRAF^{V600E}$ mutation (data not shown).

Table 1

Clinical and pathologic features of sporadic atypical Spitz tumors with epithelioid morphology

#	Age	Site	Pathologic diagnosis	Architecture	Details	Thickness (mm)	Mitoses	TILs	*BRAF V600E*	BAP1 IHC
1	23	Anterior shoulder	AST	Polypoid and compound, predominantly dermal	Sheets and nests of epithelioid cells with abundant amphophilic cytoplasm, well-defined cytoplasmic borders and vesicular nuclei exhibiting moderate pleomorphism. Scattered giant/multinucleate tumor cells.	4.5	Absent	+++	+	−
2	19	Back	AST	Dermal	Sheets and nests of large epithelioid cells with abundant amphophilic cytoplasm, well-defined cytoplasmic borders and very pleomorphic round/oval vesicular nuclei with conspicuous nucleoli. Scattered giant/multinucleate tumor cells.	2.5	Absent	+++	+	−
3	14	Scalp	AST	Compound, predominantly dermal, with congenital nevus-like pattern	Sheets and nests of epithelioid cells with abundant amphophilic cytoplasm, well-defined cytoplasmic borders and vesicular nuclei exhibiting moderate pleomorphism. Scattered giant/multinucleate tumor cells.	5.0	1/mm2, superficial	++	+	−
4	n.a.	Ear	AST	Compound, predominantly dermal, with congenital nevus-like pattern	Sheets and nests of epithelioid cells with abundant amphophilic cytoplasm, well-defined cytoplasmic borders and vesicular nuclei exhibiting moderate pleomorphism. Scattered giant/multinucleate tumor cells.	9.5	2/mm2, superficial	−	+	−
5	12	Post-auricular	AST	Compound, predominantly dermal	Sheets and nests of large epithelioid cells with abundant amphophilic cytoplasm, well-defined cytoplasmic borders and very pleomorphic round/oval vesicular nuclei with conspicuous nucleoli. Scattered giant/multinucleate tumor cells.	4.0	Absent	+++	+	−
6	44	Upper back	AST	Dermal	Sheets of large epithelioid cells with amphophilic cytoplasm, well-defined cytoplasmic borders and moderately pleomorphic vesicular nuclei with large nucleoli.	2.2	1/mm2, superficial	+	+	−
7	13	Upper back	AST	Dermal	Sheets and nests of large epithelioid cells with abundant amphophilic cytoplasm, well-defined cytoplasmic borders and mildly pleomorphic round/oval vesicular nuclei. An occasional giant/multinucleate tumor cell.	2.6	1/mm2, superficial	++	+	−
8	51	Upper back	AST	Dermal	Sheets of medium-sized epithelioid, oval and spindle cells with amphophilic cytoplasm, well-defined cytoplasmic borders and mildly pleomorphic vesicular nuclei with small nucleoli.	5.0	Absent	−	+	−

Am J Surg Pathol. Author manuscript; available in PMC 2013 June 01.

#	Age	Site	Pathologic diagnosis	Architecture	Details	Thickness (mm)	Mitoses	TILs	*BRAF V600E*	BAP1 IHC
9	59	n.a.	AST	Compound, predominantly dermal	Sheets of medium-sized epithelioid, oval and spindle cells with amphophilic cytoplasm, well-defined cytoplasmic borders and mildly pleomorphic vesicular nuclei with small nucleoli. Scattered giant/multinucleate tumor cells.	2.4	Absent	−	wt	−
10	37	Arm	AST	Dermal	Spindle and epithelioid melanocytes arranged in nests and cords. The cells contain abundant amphophilic cytoplasm and mildly pleomorphic, vesicular nuclei	3.1	2/mm2, superficial	−	+	+
11	7	Ear	AST, recurrent	Compound	Wedge-shaped tumor composed of epithelioid and spindle-shaped cells exhibiting mild cytologic atypia	2.15	1/mm2; deep	−	wt	+
12	52	Arm	AST	Dermal	Rounded superficial dermal tumor composed of plump epithelioid cells	0.6	0	−	n.a.	+
13	n.a.	Cheek	AST	Dermal	Trabeculae and sheets of moderately atypical epithelioid cells with abundant cytoplasm and conspicuous nucleoli	5.6	2/mm2; deep	++	wt	+
14	16	Ankle	AST	Dermal	Fascicles and sheets of spindle-shaped and oval melanocytes exhibiting moderate nuclear pleomorphism and large nucleoli	5.5	4/mm2, superficial	−	wt	+
15	n.a.	Thigh	AST	Compound, predominantly dermal	Sheets of epithelioid cells with abundant amphophilic cytoplasm, well-defined cytoplasmic borders and round/oval vesicular nuclei with conspicuous nucleoli; strands of dense collagen separate the tumor cells into islands of varying size; at the periphery, tumor cells merge with adjacent dermal collagen in an infiltrating pattern	2.3	2/mm2, superficial	+	wt	+
16	n.a.	Thumb	AST	Dermal	Spindle and occasional epithelioid cells with small to moderate amounts of amphophilic cytoplasm. Associated epidermal hyperplasia. Cells merge in an infiltrative fashion with dermal collagen at periphery of tumor.	2.8	4/mm2, superficial	−	wt	+
17	13	Elbow	AST, polypoid	Compound	Ulcerated tumor. Predominantly spindle cells in nests and sheets. Cells contain relatively uniform oval/spindle-shaped nuclei and small to moderate amounts of cytoplasm, with ill-defined cytoplasmic borders.	3.0	1/mm2, superficial	++	wt	+
18	12	Dorsum of foot	AST	Compound	Spindle and epithelioid cells arranged in nests and sheets separated by bundles of dermal collagen. Cells contain round to oval nuclei exhibiting little pleomorphism.	5.7	Absent	−	wt	+

#	Age	Site	Pathologic diagnosis	Architecture	Details	Thickness (mm)	Mitoses	TILs	*BRAF V600E*	BAP1 IHC
19	2	Pinna	AST	Dermal	Sheets of spindle and a few epithelioid cells containing relatively uniform oval/spindle-shaped nuclei and small to moderate amounts of amphophilic cytoplasm	6.5	2/mm2, superficial	+	wt	+
20	23	Buttock	AST	Dermal	Clusters of small epithelioid cells with small amounts of amphophilic cytoplasm and round-oval nuclei with vesicular, clumped and cleared nuclear chromatin, and conspicuous nucleoli, often irregularly-shaped	5.0	Absent	+	wt	+
21	9	Forearm	AST	Compound	Relatively uniform spindle and epithelioid cells arranged in nests and fascicles, separated by collagenous septa. Associated epidermal hyperplasia and hypergranulosis.	8.0	3/mm2	+	wt	+
22	n.a.	n.a.	AST	Compound	Epithelioid and spindle cells arranged in nests. Cells contain moderate amounts of eosinophilic cytoplasm and moderately pleomorphic nuclei with conspicuous nucleoli. Variable amounts of pigment, particularly in junctional component.	2.0	1/mm2, superficial	−	wt	+
23	14	Ear	AST	Compound, polypoid	Variably pigmented, predominantly uniform spindle cells arranged in nests and sheets. Associated extensive sclerosis of dermal component and epidermal hyperplasia.	5.7	2/mm2, superficial	−	wt	+
24	42	Buttock	AST	Compound, predominantly dermal	Sheets of variably pigmented epithelioid and spindle cells with moderate amounts of cytoplasm and moderate nuclear pleomorphism	0.85	Absent	+	wt	+
25	12	Lateral ankle	AST	Compound	Sheets and nests of variably pigmented epithelioid cells with highly pleomorphic round-oval nuclei	4.5	2/mm2	+	wt	+
26	8	Leg	AST	Predominantly dermal	Large epithelioid and spindle-shaped cells with abundant eosinophilic cytoplasm, indistinct cytoplasmic borders and moderately pleomorphic round-oval vesicular nuclei with prominent nucleoli	5.5	1/mm2, superficial	++	wt	+
27	10	Knee	AST	Dermal	Spindle and epithelioid melanocytes arranged in fascicles separated by collagenous septa. The cells contain abundant amphophilic cytoplasm with well defined cytoplasmic borders, and their nuclei are highly pleomorphic, with large and polymorphic nucleoli	2.9	3/mm2	+	wt	+
28	10	Knee	AST	Compound	Oval and spindle-shaped melanocytes with moderate amounts of amphophilic cytoplasm arranged in nests and trabeculae. Nuclei are	2.3	2/mm2	+	wt	+

#	Age	Site	Pathologic diagnosis	Architecture	Details	Thickness (mm)	Mitoses	TILs	*BRAF V600E*	BAP1 IHC
					vesicular and relatively uniform in size and shape.					
29	24	n.a.	AST	Compound	Epithelioid and oval cells with abundant amphophilic cytoplasm and round/oval, moderately pleomorphic nuclei with conspicuous nucleoli	3.3	3/mm2	++	wt	+
30	11	Upper cheek	AST	Compound	Epithelioid cells with abundant amphophilic cytoplasm, well-defined cytoplasmic borders and vesicular nuclei exhibiting moderate pleomorphism.	2.0	1/mm2, superficial	+	wt	+
31	24	Leg	AST	Compound	Predominantly nests of focally pigmented epithelioid cells with abundant amphophilic cytoplasm, well-defined cytoplasmic borders and vesicular nuclei exhibiting moderate pleomorphism and very conspicuous nucleoli. Scattered giant/multinucleate tumor cells.	1.5	2/mm2, superficial	++	wt	+
32	12	Chin	AST	Dermal	Epithelioid and oval cells with abundant amphophilic cytoplasm, well-defined cytoplasmic borders and vesicular nuclei exhibiting moderate pleomorphism. Scattered giant/multinucleate tumor cells.	1.8	1/mm2, superficial	+	wt	+

Congenital nevus-like pattern is the extension along adnexal structures

n.a., not available
TILs, tumor infiltrating lymphocytes
WT, wild type

Table 2

Comparison of clinico-pathologic features between BAP1− and BAP1+ tumors

Feature		BAP1− (n=9)		BAP1 + (n=23)		p value
		Mean/ Median	Range	Mean/ Median	Range	
Age (years)		30/21	12–59	18/12	2–52	0.046 **
Breslow thickness (mm)		4.2/4	2.2–9.5	3.6/3	0.6–6.5	NS **
Mitotic rate (per mm^2)		0	0–2	2	0−4	0.01 **
Feature	**Level**	**N**	**%**	**N**	**%**	**p value**
Anatomic site	Head/neck	3	38	6	29	0.04 †
	Trunk	4	50	2	10	
	Upper limbs	1	13	5	24	
	Lower limbs	0	0	8	38	
Architecture	Compound	0	0	11	48	0.01 †
	Dermal	4	44	9	39	
	Compound, predominantly dermal	5	56	3	13	
Predominant growth pattern	Sheet-like growth	8	89	8	35	0.02 *
	Nested growth	6	67	9	39	NS *
Cellular shape	Epithelioid cells	9	100	16	70	NS *
	Spindle/Oval cells	2	22	15	65	0.049 *
Cytoplasmic features	Cytoplasmic amphophilia	9	100	9	39	0.002 *
	Well-defined cytoplasmic borders	9	100	5	22	<0.0001 *
Nuclear features	Vesicular chromatin	9	100	7	30	0.0008 *
	Moderate pleomorphism	4	44	9	39	NS *

Feature		BAP1− (n=9)		BAP1 + (n=23)		p value
		Mean/ Median	Range	Mean/ Median	Range	
	Marked pleomorphism	2	22	2	9	NS *
	Conspicuous nucleoli	3	33	9	39	NS *
	Binucleation/multinucleation	7	78	2	9	0.0003 *
Tumor-infiltrating lymphocytes	Absent	3	33	8	35	0.02 †
	Mild	1	11	10	43	
	Moderate	2	22	5	22	
	Marked	3	33	0	0	

NS = not statistically significant (p>0.05)

** Mann-Whitney test

† Chi-squared test

* Fisher exact test

Am J Surg Pathol. Author manuscript; available in PMC 2013 June 01.

Table 3

BRAF and *BAP1* mutations in AST showing loss of BAP1 expression by IHC

Case #	*BRAF*		*BAP1*		*aCGH*
	DNA	**Protein**	**DNA**	**Protein**	**3p21 copy number status**
1	c.1799T>A	p.V600E	c.459del	p.E154Rfs*33	n.a.
2	c.1799T>A	p.V600E	wt	wt	n.a.
3	c.1799T>A	p.V600E	wt	wt	n.a.
4	c.1799T>A	p.V600E	wt	wt	n.a.
5	c.1799T>A	p.V600E	wt	wt	n.a.
6	c.1799T>A	p.V600E	c.178C>T	p.R60*	no loss
7	c.1799T>A	p.V600E	c.1768C>T	p.Q590*	no loss
8	c.1799T>A	p.V600E	c.920dup	p.N308Qfs*90	loss
9	wt	wt	c.516C>G	p.S172R	loss

n.a, not available
wt, wildtype